

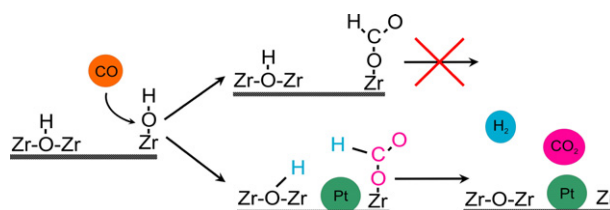


REGULAR ARTICLES

New insights in reactivity of hydroxyl groups in water gas shift reaction on Pt/ZrO₂

pp 181–187

P.O. Graf, D.J.M. de Vlieger, B.L. Mojet, L. Lefferts*

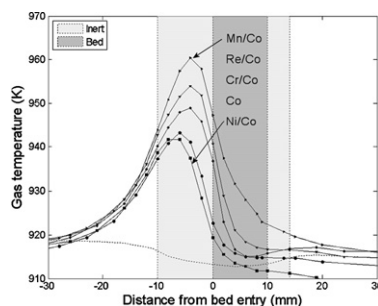


Mono-coordinated OH groups on zirconia convert to formate when exposed to CO. Formate can then decompose to CO₂ and H₂, provided both multi-coordinated OH groups and Pt are available.

Modified cobalt catalysts in the partial oxidation of methane at moderate temperatures

pp 188–198

Bjørn Christian Enger, Rune Lødeng, Anders Holmen*

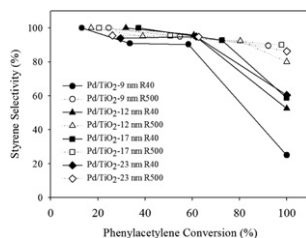


Temperature profiles from the partial oxidation of methane with air (CH₄/O₂ = 2.0) at 923 K (oven temperature) and GHSV = 15 NI CH₄/(g h). Steady state was kept for 2 h before the oven temperature was decreased with 1 K/min. The catalysts are indicated in order of appearance based on the peak maximums.

Effect of strong metal–support interaction on the catalytic performance of Pd/TiO₂ in the liquid-phase semihydrogenation of phenylacetylene

pp 199–205

Patcharaporn Weerachawanasak, Okorn Mekasuwandumrong, Masahiko Arai, Shin-Ichiro Fujita, Piyasan Praserttham, Joongjai Panpranot*

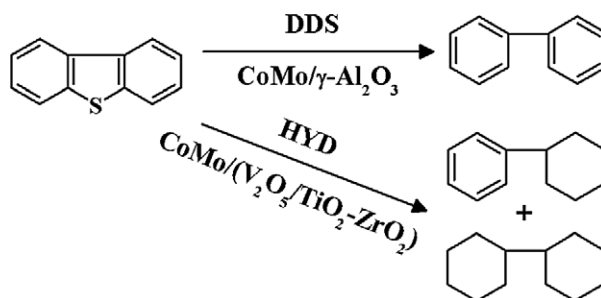


The presence of SMSI on Pd/TiO₂ catalysts when reduced at 500 °C has proven to produce great beneficial effect on both catalytic hydrogenation activities and selectivities to styrene in liquid-phase semihydrogenation of phenylacetylene under mild conditions.

Deep hydrodesulfurization over Co/Mo catalysts supported on oxides containing vanadium

pp 206–214

Chih-Ming Wang, Tseng-Chang Tsai, Ikai Wang*

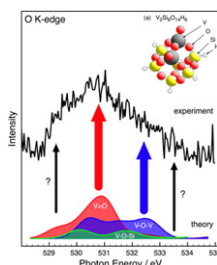


A novel catalyst support by impregnating vanadium on $\text{TiO}_2\text{-ZrO}_2$, by shifting direct desulfurization (DDS) pathway to hydrogenation (HYD) pathway for hydrodesulfurization (HDS), shows very high activity of the sterically hindered methylated dibenzothiophenes for the production of ultra low diesel.

Analysis of silica-supported vanadia by X-ray absorption spectroscopy: Combined theoretical and experimental studies

pp 215–223

M. Cavalleri, K. Hermann*, A. Knop-Gericke, M. Hävecker, R. Herbert, C. Hess, A. Oestereich, J. Döbler, R. Schlögl

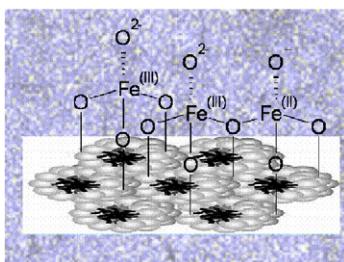


Theoretical/experimental O K-edge NEXAFS spectra for vanadia on SBA-15 show that different non-monomeric vanadia particles exist at the support surface; the presence of only monomeric species is excluded.

Insight into the properties of Fe oxide present in high concentrations on mesoporous silica

pp 224–234

A. Gervasini*, C. Messi, P. Carniti, A. Ponti, N. Ravasio, F. Zaccheria

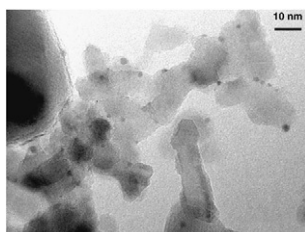


Fe oxide catalysts supported on a mesoporous, high surface area silica, with iron in a wide range of concentration ($4 < \text{Fe}_2\text{O}_3$ mass% < 17), are presented. A suite of techniques was employed to determine the structural, morphologic, surface, electronic, acidic, and red-ox properties of the samples. The samples maintained good Fe-dispersion and low metal aggregation, independently of Fe-concentration. The test reaction of isomerization of α -pinene oxide revealed the prominent presence of Lewis acid sites on all the samples.

Pd-promoted selective gas phase hydrogenation of *p*-chloronitrobenzene over alumina supported Au

pp 235–243

Fernando Cárdenas-Lizana, Santiago Gómez-Quero, Antoine Hugon, Laurent Delannoy, Catherine Louis, Mark A. Keane*

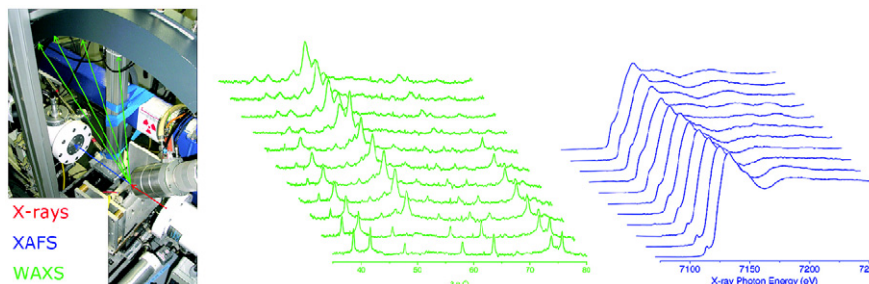


Nano-scale Au particles supported on Al_2O_3 promote 100% selective gas phase hydrogenation of *p*-chloronitrobenzene to commercially important *p*-chloroaniline; we have established that the incorporation of Pd ($\text{Au/Pd} \geq 20$, see TEM image) serves to elevate rate while retaining reaction exclusivity, an effect that we associate with bimetallic particle formation.

Local and long range order in promoted iron-based Fischer–Tropsch catalysts: A combined *in situ* X-ray absorption spectroscopy/wide angle X-ray scattering study

pp 244–256

Emiel de Smit, Andrew M. Beale, Sergey Nikitenko, Bert M. Weckhuysen*

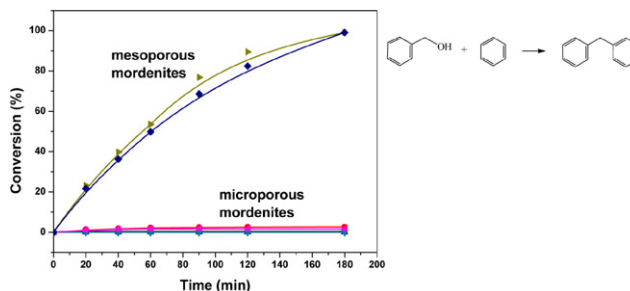


A combined *in situ* X-ray absorption and diffraction study provided new insights into the local and long range structure of iron-based Fischer–Tropsch catalysts after pretreatment and during synthesis.

Synthesis and characterization of mesoporous mordenite

pp 257–265

Xianfeng Li, Roel Prins, Jeroen Anton van Bokhoven*

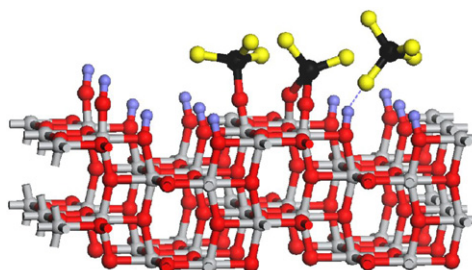


Mesoporous mordenite obtained by acid and base leaching exhibited a much higher catalytic activity in the benzylation of benzene with benzyl alcohol than conventional mordenite.

The interfacial chemistry of the impregnation step involved in the preparation of tungsten(VI) supported titania catalysts

pp 266–279

George D. Panagiotou, Theano Petsi, Kyriakos Bourikas*, Christos Kordulis, Alexis Lycourghiotis

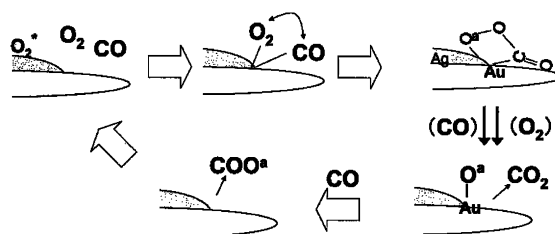


Local structures of the adsorbed W(VI) monomer oxo-species on the (1 0 0) crystal termination of anatase.

A kinetic study on the low temperature oxidation of CO over Ag-contaminated Au fine powder

pp 280–286

Yasuo Iizuka*, Tomonobu Miyamae, Takumi Miura, Mitsutaka Okumura, Masakazu Daté, Masatake Haruta

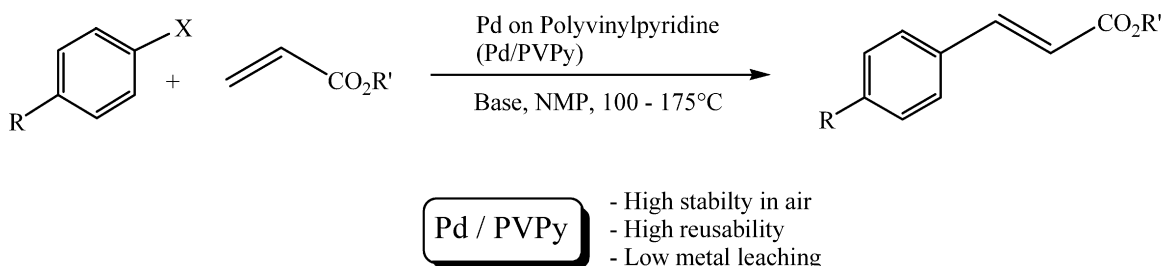


The oxidation proceeds through co-adsorption of CO and O₂ to form CO₃ succeeded by decomposition by CO and/or O₂ to produce CO₂ at contact interface of Ag and Au support.

Palladium nanoparticles supported on polyvinylpyridine: Catalytic activity in Heck-type reactions and XPS structural studies

pp 287–293

Claudio Evangelisti, Nicoletta Panziera, Paolo Pertici*, Giovanni Vitulli, Piero Salvadori, Chiara Battocchio, Giovanni Polzonetti

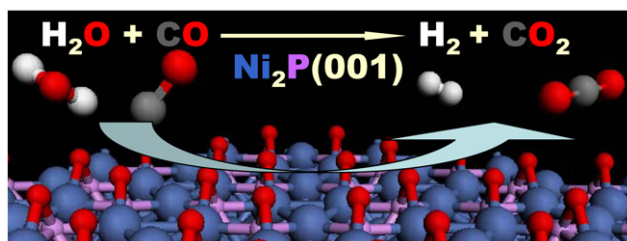


The Pd/PVPy system is very active in the Heck C–C coupling reaction. The catalyst is stable in air, can be reused several times without loss of activity and the leaching of metal in solution is negligible.

Water–gas-shift reaction on a Ni₂P(001) catalyst: Formation of oxy-phosphides and highly active reaction sites

pp 294–303

Ping Liu*, José A. Rodriguez, Yoshiro Takahashi, Kenichi Nakamura

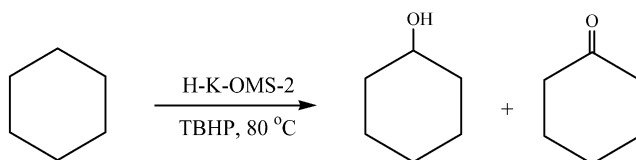


Ni₂P(001) displays a superior water–gas-shift activity. The good behavior of Ni₂P is associated with the Ni oxy-phosphides formed as a result of strong O ↔ P interactions.

Cyclohexane oxidation catalyzed by manganese oxide octahedral molecular sieves—Effect of acidity of the catalyst

pp 304–313

Ranjit Kumar, Shanthakumar Sithambaram, Steven L. Suib*

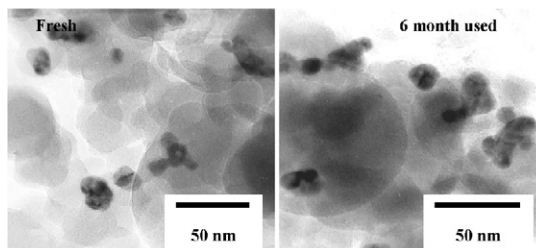


An efficient process for cyclohexane oxidation to cyclohexanol and cyclohexanone using H⁺-exchanged K-OMS-2 is reported. A dual active site mechanism has been proposed where both Lewis and Brønsted acid sites play an important role in the oxidation process.

Bimetallic PdAu–KOAc/SiO₂ catalysts for vinyl acetate monomer (VAM) synthesis: Insights into deactivation under industrial conditions

pp 314–323

Marga-Martina Pohl*, Jörg Radnik, Matthias Schneider, Ursula Bentrup, David Linke, Angelika Brückner, Ewen Ferguson



PdAu/SiO₂ vinyl acetate synthesis catalysts deactivate without any noticeable sintering for up to six months of use but do undergo considerable restructuring of the alloyed noble metal particles with time on stream.